Effect of 3D $\pi-\pi$ Stacking on Photovoltaic and Electroluminescent Properties in Triphenylamine-containing Poly(*p*-phenylenevinylene) Derivatives

Ping Shen,[†] Guangyi Sang,[‡] Junjian Lu,[†] Bin Zhao,[†] Meixiu Wan,[†] Yingping Zou,[‡] Yongfang Li,*[,‡] and Songting Tan*[,†]

College of Chemistry and Key Laboratory of Environmentally Friendly Chemistry and Applications of Ministry of Education, Xiangtan University, Xiangtan 411105, PR China, and CAS Key Laboratory of Organic Solids, Institute of Chemistry, Chinese Academy of Sciences, Beijing 100190, PR China

Received April 16, 2008; Revised Manuscript Received May 23, 2008

ABSTRACT: Poly(*p*-phenylenevinylene) (PPV) derivatives containing the 3D $\pi-\pi$ stacking structures of the triphenylamine moieties as two side chains have been synthesized by the Wittig−Horner reaction. The presence of 2,5-bis(4-(*N*,*N*-diphenylamino)phenylenevinylene units along these π-conjugated polymer backbone lowered the band gap, and thus the resulting polymers exhibited strong and broad absorption in the visible region. Triphenylamine groups effectively extended the conjugation length through 3D $\pi-\pi$ stacking and enhanced the hole-transporting properties of the polymers. Furthermore, the 3D $\pi-\pi$ stacking effects of the triphenylamine moieties on the properties of the polymer light-emitting devices (PLEDs) and photovoltaic solar cells were also investigated in detail. The maximum electroluminescence (EL) brightness of the single-layer light emitting devices for **P1** and **P2** achieved 3003 and 1697 cd/m^2, respectively. The bulk heterojunction polymer photovoltaic cells (PPVCs) based on **P1** or **P2** and PCBM (1:1, w/w) showed power conversion efficiencies up to 0.27% and 0.45% under the illumination of AM 1.5, 90 mW/cm^2, which were 3−5 times higher than that of the device based on **P3** (0.09%) without triphenylamine side chains.

1. Introduction

Poly(*p*-phenylenevinylene) (PPV) and its derivatives are one of the most attractive classes of conjugated polymers due to their high quantum yields and easy modification of the chemical structures. Recent developments in photovoltaic solar cells based on PPV derivatives in the bulk heterojunction structure have led to a significant increase in device efficiency.[1–4] The photovoltaic cells of a blend of poly(2-methoxy-5-(3,7-dimethyloctyloxy)-*p*-phenylenevinylene) (MDMO-PPV) and [6,6]-phenyl C61-butyric acid methyl ester (PCBM) have thereby proven their capacity for solar cells applications, exhibiting power-conversion efficiencies of around 2.5% for the global AM1.5 (air mass 1.5) spectrum.[5]

In the heterojunction polymer photovoltaic cells (PPVCs) based on blends of PCBM and conjugated polymers, light absorption results in the formation of excitons that dissociated at the heterojunction interface by an ultrafast electron transfer from the donor to the acceptor PCBM. Under the action of the internal electrical field, the photogenerated free holes and electrons are subsequently transported through the donor and acceptor phase to the anode and cathode, respectively. Since the holes mobility[6] of PPV neat film have previously been reported to be about 5×10^{-11} m^2 V^{-1} s^{-1}, whereas electron mobilities[7] of PCBM have been reported at 2×10^{-7} m^2 V^{-1} s^{-1}, the charge transport in a PPVCs based on these materials is strongly unbalanced. Due to the unbalanced charge transporting behavior, holes accumulate to a greater extent in the device than electrons do. The recombination probability of free charges in photovoltaic cells is increased, resulting in the relative low external photocurrent density. Therefore, the significant improvement of the hole transporting properties for the active layer in the photovoltaic solar cells could improve the balance of charge transport and then increase the power conversion efficiency of the devices.[8–12]

Triphenylamine (TPA) and its derivatives are well-known for their 3D propeller shapes and are widely used as glass-forming and hole-injecting/transporting materials for organic light-emitting diodes (LEDs).[13–17] Kido and his co-workers first reported a new PPV derivative substituted with monotriphenylamines, which emitted yellow light with the maximum luminance over 29 000 cd/m^2 under a low driving voltage (8 V).[18] Most of the novel conjugated polymers with triphenylamine derivatives on the main chain exhibited their potential applications in fields of the PPVCs.[19–21] PPV derivatives containing the 3D structures of the triphenylamine moieties as two side chains could provide another perspective for the preparation of the new photovoltaic materials. So it is of interest to synthesize these kinds of efficient photovoltaic PPV materials, which could broaden the absorption range and improve the power conversion efficiency.

In this paper, we have synthesized two new PPV derivatives (**P1** and **P2**) containing 3D $\pi-\pi$ stacking structures. Two triphenylamine groups were attached directly as the two side chains of phenylenevinylene backbones so that the electronic and physical properties of the polymers could be further tunable. For comparison, the poly(*p*-phenylenevinylene) (**P3**) without triphenylamine side groups was also synthesized. The polymer light-emitting devices (PLEDs) and PPVCs based on **P1**, **P2**, and **P3** were fabricated and evaluated to investigate the light-emitting and photovoltaic properties. Furthermore, the 3D $\pi-\pi$ stacking effects of the triphenylamine moieties on the thermal, optical absorption, fluorescence, electrochemical properties of the PPV derivatives were also investigated in detail.

2. Experimental Section

2.1. Materials. 4-methoxyphenol, tetrabutylammonium bromide, potassium carbonate, paraformaldehyde, sodium bromide, 2,5-dibromo-*p*-xylene, *N*-(4-bromophenyl)-*N*,*N*-diphenylamine and *n*-

* Corresponding authors.
[†] College of Chemistry and Key Laboratory of Environmentally Friendly Chemistry and Applications of Ministry of Education, Xiangtan University.
[‡] CAS Key Laboratory of Organic Solids, Institute of Chemistry, Chinese Academy of Sciences.

10.1021/ma800847f CCC: $40.75
Published on Web 06/28/2008

buthyllithium were purchased from Alfa Aesar and Shanghai Medical Company (China), respectively. All other reagents were used as received from commercial sources, unless otherwise stated.

2.2. Measurements. ^{1}H NMR spectra were collected on a Bruker AVANCE 400 spectrometer. FT-IR spectra were obtained on a Perkin-Elmer Spectra One, and UV spectra were measured on a Perkin-Elmer Lamada 25 spectrometer. Thermogravimetric analyses (TGA) were performed under nitrogen at a heating rate of 20 °C/min with a Netzsch TG 209 analyzer. Differential scanning calorimetric measurements (DSC) of the polymers were performed under nitrogen at a heating rate of 20 °C/min with a TA DSC Q10 instrument. The average molecular weight and polydispersity index (PDI) of the polymers were determined using Waters1515 gel permeation chromatography (GPC) analysis with THF as eluent and polystyrene as standard. The PL spectra of the polymers were obtained using Perkin-Elmer LS-50 luminescence spectrometer. The cyclic voltammograms of thin films of the polymers were done by using EG&G Princeton Applied Research Model 273 potentiostat/galvanostat equipped with Electrochemical Analysis System software. Platinum wires were used as both the counter and working electrodes, and saturated calomel electrode (SCE) was used as a reference electrode. Thin films of the polymers on platinum electrodes were prepared by dipping the electrode into a 0.2−1.0 wt % polymer solution. The measurements were conducted in a 0.1 M Bu_4NClO_4 acetonitrile solution using at a scan rate of 50 mV/s at room temperature. Current−voltage measurements of the devices were conducted on a computer-controlled Keithley 236 source measure unit. A xenon lamp with an AM1.5 filter was used as the white-light source, and the optical power at the sample was 90 mW/cm^2.

2.3. Light Emitting Device Fabrication. The single-layered polymer light-emitting diodes (PLEDs) with the configuration ITO/PEDOT/polymer/Ca/Al were fabricated. ITO-coated glass substrates were first thoroughly cleaned in an ultrasonic solvent bath and then dried in a heating chamber at 120 °C. Poly(ethylenedioxythiophene) (PEDOT) was spin-coated on the ITO glasses at a speed of 3000 rps for 60 s and then baked for 15 min at 120 °C to give a thin layer film of about 50 nm thick. The light-emitting polymer layer was then deposited onto the film by spin-coating a polymer solution in toluene (10 mg/mL) at a speed of 1500 rps for 60 s. Uniform and pinhole-free films with thicknesses around 70−80 nm could be readily obtained. Finally, a thin layer of calcium (about 4 nm) and a layer of aluminum (about 100 nm) were deposited in sequence in a vacuum thermal evaporator through a shadow mask, yielding active areas of 16 mm^2. For device characterizations, current−voltage-brightness ($J-V-B$) was measured using a Keithley 2400/2000 current/voltage source unit with a calibrated silicon photodiode. All the above processes and measurements were carried out in the open air and at room temperature.

2.4. Fabrication and Characterization of Polymer Solar Cells. The PPVCs was constructed in the traditional sandwich structure through several steps. Poly(3,4-ethylene dioxythiophene)−poly(styrene sulfonate) (PEDOT:PSS, from Bayer AG) was spin-coated from an aqueous solution on a cleaned indium tin oxide (ITO)/glass substrate giving a thickness of about 30 nm as measured by Ambios Technology XP-2 surface profilometer, and it was dried subsequently at 150 °C for 10 min. The photosensitive blend layer of polymer and PCBM was prepared by spin-coating the chlorobenzene solution of the polymers and PCBM (1:1 w/w) with the polymer concentration of 12 mg/mL on the ITO/PEDOT:PSS electrode, and dried at 80 °C for 30 min, in a nitrogen-filled glovebox. The cathode of devices, consisting of 1 nm of LiF and 150 nm of aluminum, was thermally deposited on the top of polymer film at 5×10^5 Pa. The active area of the device is 4 mm^2. Current density−voltage ($J-V$) characteristics were measured by a computer controlled Keithley 236 source measurement unit in dark and under AM1.5 illumination conditions, 90 mW/cm^2. All these measurements were performed under ambient atmosphere at room temperature.

2.5. Synthesis of the Monomers and Polymers. The synthetic routes of the monomers and polymers were shown in Scheme 1. The detailed synthetic procedures were as follows.

*1-Methoxy-4-octoxybenzene (***1a***).* A solution of 4-methoxyphenol (2.48 g, 20 mmol), 1-bromooctane (3.86 g, 20 mmol), and potassium carbonate (3.04 g, 22 mmol) in DMSO (60 mL) was stirred and heated at 140 °C under nitrogen overnight. The mixture was then poured into 200 mL of distilled water after being cooled to room temperature. The crude product was washed several times with aqueous sodium carbonate solution and water then recrystallized from isopropanol. After filtration and drying in a vacuum oven, a white pastelike crystal was obtained with mp 34−35 °C. Yield: 87%. ^{1}H NMR ($CDCl_3$, 400 MHz): δ (ppm) 6.71 (m, 4H), 3.80 (t, 2H), 3.62 (s, 3H), 1.76 (m, 2H), 1.42−1.28 (m, 10H), 0.90 (t, 3H). Anal. Calcd for $C_{15}H_{24}O_2$: C, 76.23; H, 10.24. Found: C, 76.12; H, 10.25.

The synthetic procedure for **1b** was similar to that for **1a**, giving a white pastelike crystal. Yield: 80%.

^{1}H NMR ($CDCl_3$, 400 MHz): δ (ppm) 6.76 (s, 4H), 3.93 (t, 4H), 3.8−3.75 (t, 8H), 1.72−1.40 (m, 8H), 0.93 (t, 6H). Anal. Calcd for $C_{22}H_{38}O_2$: C, 78.89; H, 11.45. Found: C, 78.90; H, 11.47.

*1,4-Bis(bromomethyl)-2-methoxy-5-octoxybenzene (***2a***).* A three-necked flask containing 1-methoxy-4-octoxy benzene (2.36 g, 10 mmol), paraformaldehyde (1.05 g, 35 mmol), sodium bromide (3.50 g, 34 mmol), and glacial acetic acid (15 mL) was placed in an ice bath. Then sulfuric acid (3.3 mL, 33 mmol) and isochoric glacial acetic acid (50%, V/V) were carefully added into this flask, and the mixture was stirred for 24 h at 60−70 °C. The pale yellow solid was precipitated in water and recrystallized from hexane twice to obtained compound **2** as a white crystal with mp 82−83 °C. Yield: 78%. ^{1}H NMR ($CDCl_3$, 400 MHz): δ (ppm) 7.00 (s, 2H), 4.72 (s, 4H), 4.06 (t, 2H), 3.84 (s, 3H), 1.80−1.64 (m, 2H), 1.38−1.25 (m, 10H), 0.90 (t, 3H). Anal. Calcd for $C_{17}H_{26}Br_2O_2$: C, 48.36; H, 6.21. Found: C, 48.40; H, 6.25.

The synthetic procedure for **2b** was similar to that for **2a**, giving a white crystal. Yield: 75%. ^{1}H NMR ($CDCl_3$, 400 MHz): δ (ppm) 7.01 (s, 2H), 4.61 (s, 4H), 4.06 (t, 4H), 1.86 (m, 4H), 1.55 (m, 4H), 1.36 (m, 8H), 0.96 (t, 6H). Anal. Calcd for $C_{24}H_{40}Br_2O_2$: C, 55.39; H, 7.75. Found: C, 55.42; H, 7.79.

*1,4-Bis(diethylphosphonatomethyl)-2,5-dioctoxybenzene (***3b***).* A mixture of 1,4-bis(bromomethyl)-2,5-dioctoxybenzene (4.15 g, 7.98 mmol) and triethyl phosphite (10.25 g, 61.68 mmol) was heated to 90 °C for 16 h. Excess triethyl phosphite was separated by vacuum distillation. Hexane (25 mL) was added, and the reaction was stirred at 50 °C for 30 min. The solvent was removed by vacuum distillation. The product was obtained as a thick oil. Yield: 98%. ^{1}H NMR ($CDCl_3$, 400 MHz): δ (ppm) 7.0 (d, 2H), 4.07 (m, 8H), 3.93 (t, 4H), 3.26−3.18 (m, 4H), 1.82 (m, 4H), 1.50−1.25 (m, 20H), 1.25 (t, 12H), 0.90 (t, 6H).

The synthetic procedure for **3a** was similar to that for **3b**, giving a thick oil. Yield: 98%. ^{1}H NMR ($CDCl_3$, 400 MHz): δ (ppm) 6.93 (s, 1H), 6.90 (s, 1H), 4.05 (m, 8H), 3.93 (t, 2H), 3.79 (s, 3H), 3.26−3.18 (m, 4H), 1.78−1.72 (m, 2H), 1.44−1.28 (m, 10H), 1.25 (t, 12H), 0.90 (t, 3H).

*2,5-Dibromoterephthalaldehyde (***4***).* Sulfuric acid (10 mL) was added into a suspension containing 2,5-dibromo-*p*-xylene (2 g, 75.76 mmol), acetic acid, and acetic anhydride at 0 °C. CrO_3 (4.19 g, 58.33 mmol) powder was added into the resulting mixture group by group. The reaction temperature was controlled under 10 °C. After being stirred at 0 °C for about 5 h, the mixture was poured into the ice-cold water and washed with water. The solid product was filtered and washed with ice-cold methanol. The obtained powder was vacuumed and recrystallized from methanol to give yellow crystal with mp 178−179 °C. Yield: 35%. ^{1}H NMR ($CDCl_3$, 400 MHz): δ (ppm) 10.31 (s, 2H), 8.15 (s, 2H). Anal. Calcd for $C_8H_4Br_2O_2$: C, 32.91; H, 1.38. Found: C, 32.60; H, 1.52.

*2,5-Bis(4-(N,N-Diphenylamino)phenyl)terephthalaldehyde (***5***).* **4** (2.744 g, 9.43 mmol), Pinacol(4-(*N*,*N*-diphenylamino)phenyl)boronate (7.002 g, 18.86 mmol), and K_3PO_4 (2.50 g, 11.8 mmol) were dissolved in DMF (47 mL). $Pd[P(Ph)_3]_4$ (181 mg, 0.157 mmol) was added into the solution at 60 °C under nitrogen. The mixture

Scheme 1. Synthetic Routes of the Monomers and Polymers

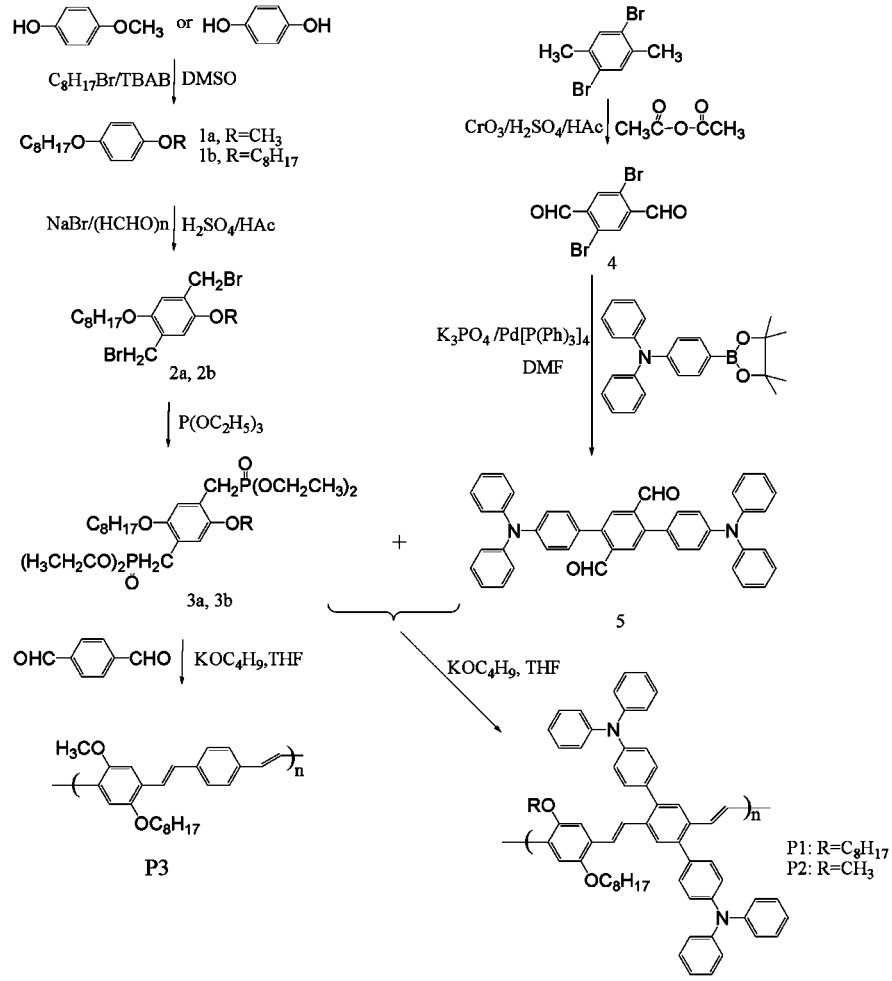

was stirred at 100 °C for 15 h and then extracted with dichloromethane. The organic layer was washed with water, dried over anhydrous sodium sulfate, filtered and evaporated. The crude product was purified using a silica gel column with hexane/dichloromethane (5/1, v:v) eluent and recrystallized from hexane to give an orange solid (2.34 g, yield 40%). ^{1}H NMR ($CDCl_3$, 400 MHz): δ (ppm) 10.16 (s, 2H), 8.08 (s, 2H), 7.33 (d, 4H), 7.28−7.09(m, 24H). Anal. Calcd for $C_{44}H_{32}N_2O_2$: C, 85.14; H, 5.20; N, 4.51. Found: C, 85.66; H, 5.16; N, 4.51.

Poly[1,4-dioctoxylphenylenevinylene-alt-2,5-bis(4-(N,N-diphenylamino)phenylenevinylene] (**P1**). **3b** (3.043 g, 4.8 mmol) and **5** (2.976 g, 4.8 mmol) was dissolved in 60 mL of anhydrous THF. Twelve mL of potassium tert-butoxide (1.0 M THF solution, 12 mmol) was added into the solution over 30 min using the syringe pump. The reaction mixture was stirred for 12 h at room temperature, and then the solution was heated at 60 °C for 12 h. The polymerization solution was poured into 60 mL of methanol, filtered and vacuum-dried to give a bright red solid. IR (KBr): 958 cm^{-1} (m, trans HC═CH). ^{1}H NMR ($CDCl_3$, 400 MHz): δ (ppm) 7.68 (s, 2H), 7.31 (d, 4H), 7.22−6.98 (m, 24H), 7.10 (d, 2H), 6.88 (s, 2H), 3.87 (m, 4H), 1.67 (m, 4H), 1.37−1.05 (m, 20H), 0.74 (m, 6H). Anal. Calcd for $(C_{68}H_{71}N_2O_2)_n$: C, 86.25; H, 7.50; N, 2.95. Found: C, 86.66; H, 7.16; N, 2.55.

Poly[1,4-(2-methoxy-5-octyoxyl)phenylenevinylene-alt-2,5-bis-(4-(N,N-diphenylamino)-phenylenevinylene] (**P2**). The synthetic procedure for **P2** was similar to that of **P1**, giving a red solid. IR (KBr): 958 cm^{-1} (m, trans HC═CH). ^{1}H NMR ($CDCl_3$, 400 MHz): δ (ppm) 7.7 (s, 2H), 7.31 (d, 4H), 7.22−6.98 (m, 24H), 7.10 (d, 2H), 6.87 (s, 2H), 4.05 (m, 2H), 3.73 (s, 3H), 1.67 (m, 2H), 1.37−1.05 (m, 12H), 0.74 (m, 3H). Anal. Calcd for $(C_{61}H_{56}N_2O_2)_n$: C, 86.32; H, 6.60; N, 3.30. Found: C, 85.66; H, 6.57; N, 3.40.

3. Results and Discussion

3.1. Synthesis and Characterization. The synthetic routes of the monomers and corresponding polymers were shown in Scheme 1. Pinacol(4-(*N*,*N*-diphenylamino)phenyl)boronate was synthesized according to the reported literature.[22] Compound **4** was synthesized from 2,5-dibromo-*p*-xylene under the oxidation of CrO_3 in the mixture of acetic acid and acetic anhydride. The key intermediate, monomer **5**, was synthesized from monomer **4** and pinacol(4-(*N*,*N*-diphenylamino)phenyl)boronate in 40% yield according to the Suzuki coupling reaction, and purified using a silica gel column with a hexane/dichloromethane (5/1, v:v) eluent. The obtained polymers were prepared according to the Wittig−Horner polymerization methods.

The structures of polymers were confirmed by ^{1}H NMR and FT-IR. The disappearance of the characteristic proton peaks −CHO at around 10.0 ppm for monomers and the appearance of new vinylic proton peaks at 7.1 ppm with aromatic proton peaks in polymers confirmed the polymerization reaction. The presence of absorption at 958 cm^{-1} in the FT-IR spectra of polymers indicated that the olefin groups were predominantly in the trans-configuration.[23] The polymers were soluble in common organic solvents, such as chloroform, toluene, and xylene at room temperature and were easily spin-coated onto the indium−tin oxide (ITO) coated glass substrates. The weight-average molecular weights of **P1**, **P2**, and **P3** were 1.1×10^4, 2.0×10^4, and 1.2×10^4, with polydispersity indexes of 1.76, 1.60, and 2.10, respectively. The polymerization results of polymers were summarized in Table 1. Before the fabrication of the devices, the crude polymers were dissolved in chloroform

Table 1. Polymerization Results and Thermal Properties of the Polymers

polymers	yield (%)	M_w ($\times 10^4$)[a]	PDI	TGA[b] (°C)	T_g[c] (°C)
P1	35	1.1	1.76	300	90
P2	40	2.0	1.60	400	120
P3	45	1.2	2.10	380	62

[a] Determined by GPC in THF based on polystyrene standards. [b] Temperature at 5% weight loss under nitrogen. [c] Determined by DSC at a heating rate of 20 °C/min under nitrogen.

Table 2. UV, PL Spectral Data, and Electrochemical Properties of the Polymers

	solution λ_{max} (nm)[a]		film λ_{max} (nm)[b]		E_g^{opt}	HOMO	LUMO
polymers	UV	PL	UV	PL	(eV)[c]	(eV)[d]	(eV)[d]
P1	460	529	471	576	2.25	−5.05	−3.00
P2	470	535	481	576	2.00	−5.0	−2.89
P3	458	510	447	527	2.29	−5.47	−2.90

[a] Measured in chloroform solution. [b] Polymer cast from chloroform solution. [c] Band gap estimated from the onset wavelength of optical absorption. [d] Energy levels calculated from the cyclic voltammograms.

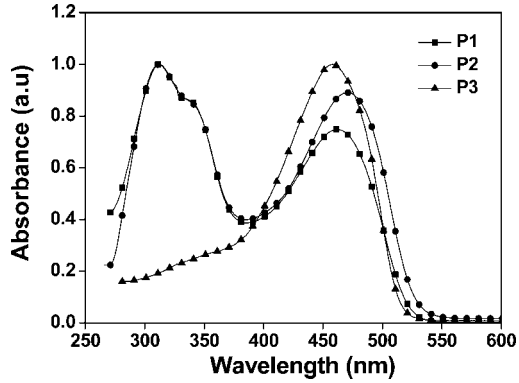

Figure 1. UV−vis absorption spectra of the polymers in the diluted $CHCl_3$ solution.

and precipitated from ethanol in order to remove the unreacted monomers and oligomers.

3.2. Thermal Properties. The thermal properties of polymers were obtained by thermogravimetric analysis (TGA) and differential scanning calorimetry (DSC) measurements. The TGA curves of polymers exhibited high thermal stability and the onset weights loss temperature were found to be 300, 400 and 380 °C for **P1**, **P2**, and **P3**, respectively. Synchronously, the glass transition temperatures (T_g) of **P1**, **P2**, and **P3** were observed to be 90, 120, and 62 °C, and no crystallizing or melting peaks were detected. The results indicated that the polymers were amorphous. It was clear that the introduction of rigid groups in the side chains in conjugated polymers can benefit to improve the thermal stability. The high thermal stability of the EL polymers could benefit to increase the stability of the PPVCs and PLEDs, which prevents morphological change, deformation, and degradation of the active layer by current-induced heat during the operation of the photovoltaic polymers.[24]

3.3. Optical Properties. The photophysical properties of the polymers were investigated by UV−vis and fluorescence spectroscopy in diluted $CHCl_3$ solution (10^{-3} mol/L) and thin films on quartz plates. The UV−vis absorption and photoluminescence properties of the polymers were summarized in Table 2. Figure 1 shows the UV−vis absorption spectra of **P1**, **P2**, and **P3** in diluted $CHCl_3$ solution. The results showed two optical absorption bands centered at 300 and 480 nm for **P1** and **P2**. The first absorption peaks in the short wavelength region at 300 nm were attributed to the n−π* electronic absorption bands of the triphenylamine moiety. The second absorption peaks at 480 nm were ascribed to the $\pi-\pi$* transition bands of

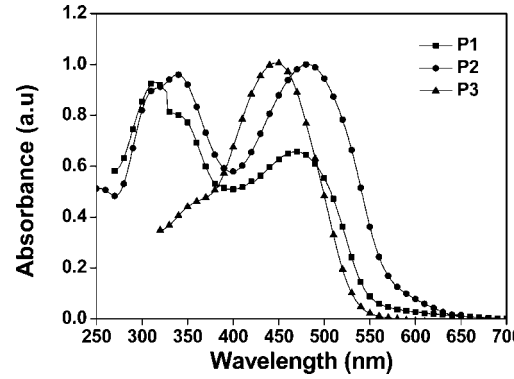

Figure 2. UV−vis absorption spectra of the polymers in thin films.

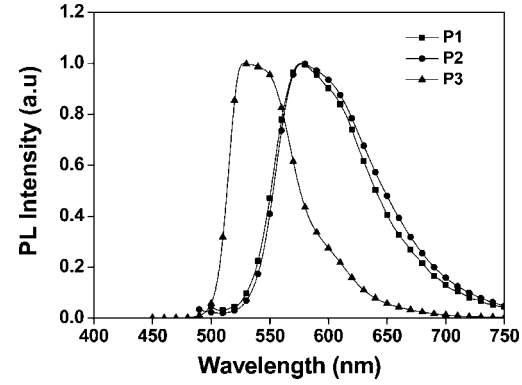

Figure 3. Photoluminescence spectra of the polymers in the thin films.

the main-chain backbone. **P3** exhibited only one $\pi-\pi$* transition band (λ_{max} = 447 nm) derived from the absorption of the polymer backbone. In comparison with the solution absorption spectra, as shown in Figure 2, the absorption edge of polymers **P1** and **P2** in thin films red-shifted about 25 and 30 nm, respectively. This can be explained as the enhancement of the intherchain interaction in the solid states. The two absorption bands centered 300 and 480 nm exhibited comparable absorption intensity for **P2** in thin film compared with that of **P1**. It can be explained that the two long alkoxyl groups could induce the twist of the polymer backbone, which decreased the aggregation effect in the solid film. In comparison with **P3**, the maximum absorption peaks of thin film absorption spectra of **P1** and **P2** showed red-shifts about 24 and 34 nm, respectively. The results indicated that the effective conjugated length increased for **P1** and **P2** through 3D $\pi-\pi$ stacking. The band gaps of **P1**, **P2**, and **P3** was 2.25, 2.0 and 2.29 eV, which was calculated from the absorption onset wavelengths (λ_{onset}) using the equation as $1240/\lambda_{onset}$. From the absorption properties of polymers, as we expected, **P1** and **P2** were used prior to **P3** for the application of photovoltaic cells for the introduction of the triphenylamine side chains.

The photoluminescence (PL) spectra of polymers were measured in the diluted $CHCl_3$ solution (10^{-5} mol/L) and thin films on quartz plates (shown in Table 2 and Figure 3). The PL spectra of **P1**, **P2**, and **P3** have presented the maximum emission peaks at 550, 560 and 510 nm in $CHCl_3$ solution, respectively. The solid film PL spectra of **P1** and **P2** showed a main peak at 575 and 580 nm with a shoulder peak at 610 and 620 nm, respectively. The maximum emission peak of thin film spectrum of **P2** was red-shifted about 50 and 24 nm in comparison with that of **P3** and the PPV derivative reported by Kido, respectively.[18] These results indicated that the aggregation of the polymers could be further enhanced through the 3D $\pi-\pi$ stacking of the two triphenylamine groups directly attached as

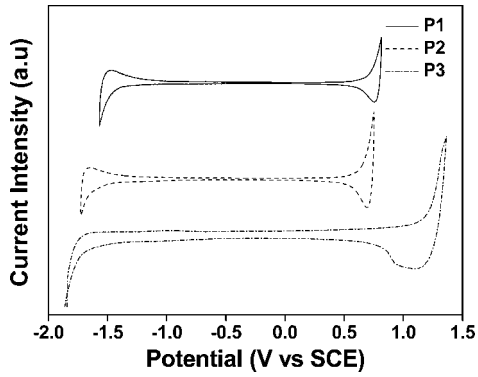

Figure 4. Cyclic voltammograms of the polymers film on platinum electrode in 0.1 mol/L Bu_4NClO_4 acetonitrile solution.

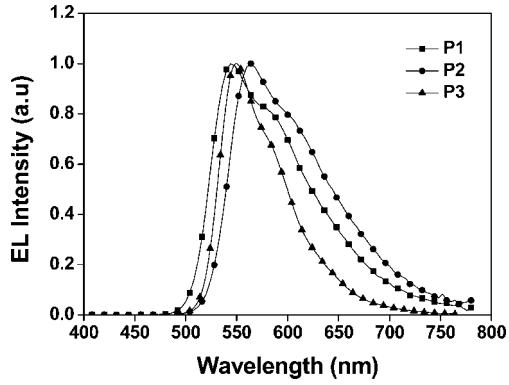

Figure 5. EL spectra of the polymers with a configuration of ITO/PEDOT/polymers/Ca/Al under the driving voltage of 10 V.

the two side chains of phenylenevinylene backbones. Under irradiation of 300 nm attributed to the triphenylamine moiety, **P2** also showed a strong PL emission at the same wavelength (560 nm), and its PL intensity was higher than that under the excitation of the PPV backbone. The results indicated that energy transfer occurs from the conjugated side groups to the polymer main chains after the conjugated side chains absorb the photons in the wavelength rang 300−350 nm. The phenomenon ensures that all photons absorbed by the polymers are useful for the photovoltaic conversion.

3.4. Electrochemical Properties. To investigate the information on the charge injection, a cyclic voltammogram (CV) was used to estimate the HOMO and LUMO energy levels of the polymers. For comparison, energy band diagram (E_g^{opt}) of polymers determined from an optical absorption spectrum was also listed in Table 2. The HOMO and the LUMO were measured by electrochemical CV, when SCE electrode was used as the reference electrode, the correlation can be expressed as[25,26]

$$E_{HOMO} = -e(E_{ox} + 4.4)\ (eV)$$

$$E_{LUMO} = -e(E_{red} + 4.4)\ (eV)$$

As observed from Figure 4, neither the reduction nor the oxidation CVs of the polymers showed reversible processes. The onset potentials for oxidation (E_{ox}^{onset}) were observed to be 0.65, 0.60 and 1.07 for **P1**, **P2** and **P3**. On the other hand, the onset potentials for reduction (E_{red}^{onset}) were found to be −1.40, −1.51, and −1.50. From the values of E_{ox}^{onset} and E_{red}^{onset}, the HOMO and LUMO energy levels of polymers were calculated, and the results are shown in Table 2. The HOMO energy levels of **P1** and **P2** attributed to the introduction of triphenylamine moieties were reduced in comparison with **P3**, indicating that hole-injection and transporting properties have been improved.

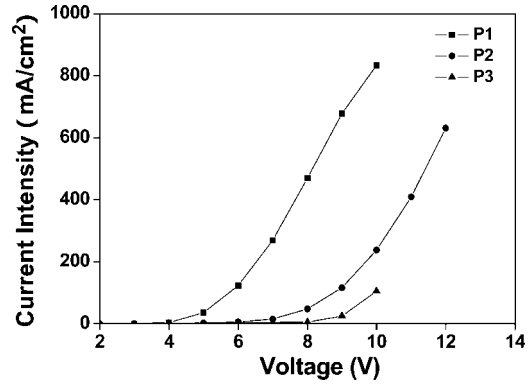

Figure 6. Current density−voltage characteristics of the ITO/PEDOT/polymers/Ca/Al devices.

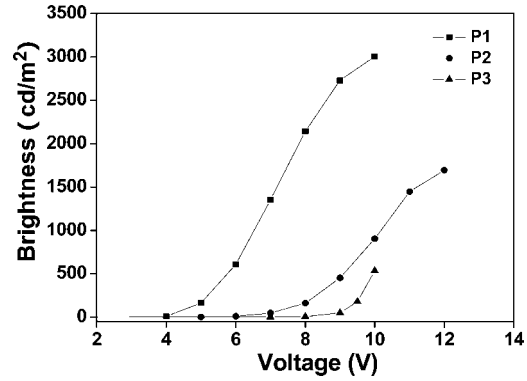

Figure 7. Luminance−voltage characteristics of the ITO/PEDOT/polymers/Ca/Al devices.

The result was reasonable for the effect of the electron-rich triphenylamine groups on the electronic properties of the conjugated polymer chains. The electrochemical band gap (E_g^{EC}) calculated from CV data was within the range of error (0.2−0.5 eV) in comparison with E_g^{opt}.[27]

3.5. Photovoltaic Properties. The bulk heterojunction solar cells based on the polymers in combination of the well-known fullerene acceptor PCBM have been prepared and investigated. The employed device structure was ITO/PEDOT:PSS/polymer:PCBM/LiF/Al. The current−voltage ($J-V$) curves were measured in dark and under illumination from solar simulator at 90 mW/cm^2 light intensity, and the results are shown in Figure 8 and listed in Table 4. The energy conversion efficiency under the incident light and the fill factor were calculated using eqs 1 and 2

$$\eta = V_{max}J_{max}/P_{input} \quad (1)$$

$$FF = V_{max}J_{max}/V_{oc}J_{sc} \quad (2)$$

where V_{oc} [mV], J_{sc} [mA cm^{-2}], FF, and P_{input} [mW cm^{-2}] were the open-circuit potential, short-circuit current density, fill factor, and incident-light power, respectively. V_{max} [mV] and J_{max} [mA cm^{-2}] were the voltage and current density at the point of the maximum power output, respectively.

Figure 8 shows $J-V$ curves of the PPVCs, and Table 4 lists the corresponding V_{oc}, J_{sc}, FF, and energy conversion efficiency. As the J_{sc} was determined from the amount of absorbed light and by the internal conversion efficiency.[28,29] As we expected, the J_{sc} would be higher for the device **P2** than that for device **P1**. It was clear that the J_{sc} of the PPVCs based on **P2** reached to 1.2 mA/cm^2, which increased by 43% as compared with that based on **P1**. The V_{oc} of the PPVC/**P2** (0.89 V) was a little higher than that of PPVC/**P1** (0.77 V). The slight increase of

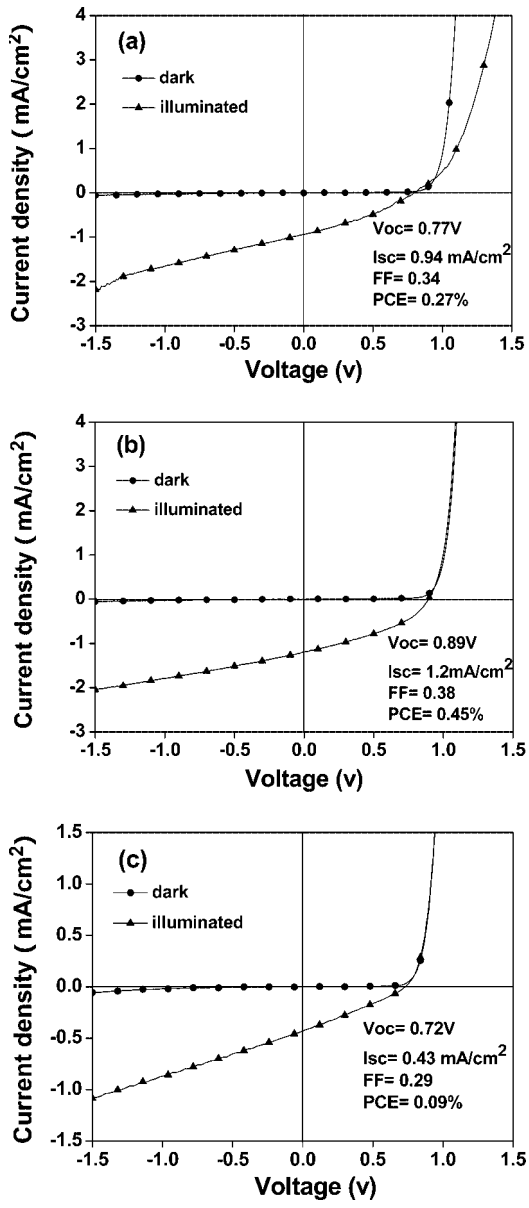

Figure 8. $J-V$ curves of the polymer solar cells based on **P1** (a), **P2** (b), and **P3** (c) under the illumination of AM 1.5, 90 mW/cm^2.

Table 3. EL Spectral Data, Luminance, and EL Efficiency of the Polymers

polymers	EL λ_{max} (nm)	turn-on voltage (V)	luminescence (cd/m^2)	EL efficiency (cd/A)
P1	544	4	3003	0.50
P2	565	5	1697	0.39
P3	548	6	534	0.04

Table 4. Photovoltaic Properties of the Polymer Solar Cells of the Polymers under the Illumination of AM 1.5, 90 mW/cm^2

polymers	V_{oc} (V)	I_{sc} (mA/cm^2)	FF (%)	PCE (%)
P1	0.77	0.84	34	0.27
P2	0.89	1.2	38	0.45
P3	0.72	0.43	29	0.09

the V_{oc} for the device **P2** could be explained by the larger interfacial area for exciton charge separation due to the good dispersion of PCBM in the polymer **P2** matrix.[30] The fill factor related to the lower series resistance of the photovoltaic device, were 0.34 and 0.38 for **P1** and **P2**, respectively.

The power conversion efficiency of the PPVC/**P2** (0.45%) was increased by 67% in comparison with that of the PPVC/**P1** (0.27%). Compared with the device **P1**, the improved power conversion efficiency of the PPVCs based on the **P2** can be benefited from its higher open circuit voltage and broad absorption range. To further evaluate the effect of triphenylamine moieties on the solar cells properties, the bulk heterojunction solar cells based on **P3** were also fabricated with **P3** and PCBM blends in a ratio of 1:1. As shown in Figure 8c, the J_{sc}, V_{oc}, FF, and PCE of the PPVC based on **P3** were 0.43 mA/cm^2, 0.72 V, 0.29, and 0.09%. These results clearly indicated that the power conversion efficiency was significantly improved for **P1** and **P2** due to the extended conjugated side chain with the introduction of the triphenylamine moieties by 3D $\pi-\pi$ stacking and the improvement of hole-transporting properties. Given the low values of the current density listed in Table 4, it is likely that the photovoltaic performance can be further improved by optimizing the polymerization conditions to improve polymer purity and molecular weight, the ratio of the polymer to PCBM, and/or device fabrication processes.

3.6. Light Emitting Properties. The EL properties of polymers were investigated by fabricating the single-layer PLEDs of ITO/ PEDOT/polymer/Ca/Al. The light emitting characteristics of the polymers were summarized in Table 3. Figure 5 shows the EL spectra of polymers under the driving voltage of 10 V. The PLEDs using **P1** and **P2** as the emissive layer emitted yellow light with the maximum emission peaks at 544 and 565 nm, respectively. The color stability under different voltages for **P1** and **P2** was also investigated. The CIE coordinates based on device **P1** under different voltages of 8, 10, and 12 V were (0.433, 0.551), (0.422, 0.558), and (0.416, 0.563), respectively. The EL spectra of **P2** were almost same with the CIE coordinates of (0.503, 0.492), (0.500, 0.494), and (0.496, 0.498) under different voltages, and showed better color stability than **P1**. We have reported the EL properties of **P3** without triphenylamine side chains.[31] The PLEDs based on **P3** emitted yellow light with the maximum emission peaks at 548 nm and the maximum brightness of 534 cd/m^2. The device based on **P1** showed the maximum brightness of 3003 cd/m^2, two times higher than that of device **P2**. That may be because the long alkoxyl groups with a high concentration could decrease the quenching effect of triphenylamine moieties in the solid states. Owing to the introduction of triphenylamine moieties side chains, the maximum brightness of **P2** was 1697 cd/m^2, which was about three times higher than that of **P3**. The different PLED performances between **P2** and the PPV derivative reported by Kido could be attributed to the difference of the molecular weight, the HOMO and LUMO energy levels of polymers and device fabrication condition.[18] As shown in Figure 6, the two polymers **P1** and **P2** exhibited excellent conductivity as the current intensity reached 833 and 630 mA/cm^2 for **P1** and **P2** at 10 V, respectively. Under the driving voltage of 8 V, the current based on the device **P1** was three times higher than **P2**, indicating a higher current resistance in the **P2**-based device.[32]

4. Conclusions

In summary, two triphenylamine-containing PPV derivatives were synthesized and characterized. The 3D $\pi-\pi$ stacking structures of the triphenylamine moieties effects on the photophysical properties of the PPV derivatives have been extensively studied. The appearance of the absorption peak around 300 nm, the strengthening of absorption intensity around 480 nm, and the pronounced red-shifts upon the formation of the corresponding solid films implied that the effective conjugated length of polymer backbone was increased due to the 3D $\pi-\pi$ stacking of the electron-rich triphenylamine moieties along the phenylenevinylene backbone. The maximum EL brightness of the single-layer light emitting device for **P1** and **P2** achieved 3003

and 1697 cd/m^2, respectively. The best PPVCs performance was obtained from the device based on **P2** with an open-circuit voltage of 0.89 V, a short-circuit current density of 1.20 mA/cm^2, and an overall power conversion efficiency of 0.45%, which was five times higher than that of the device based on **P3** (0.09%) without triphenylamine side chains. The improved power conversion efficiency of the PPVCs based on the triphenylamine-containing polymers could be attributed to the relative higher open circuit voltage and broader absorption region.

Acknowledgment. This work was supported by the National Nature Science Foundation of China (Grant Nos. 50473045 and 50633050) and key project of Hunan Province of China.

References and Notes

(1) Colladet, K.; Fourier, S.; Cleij, T. J.; Lutsen, L.; Gelan, J.; Vanderzande, D.; Huong Nguyen, L.; Neugebauer, H.; Sariciftci, S.; Aguirre, A.; Janssen, G.; Goovaerts, E. *Macromolecules* **2007**, *40*, 65.
(2) Cho, N. S.; Park, J. H.; Lee, S. K.; Lee, J.; Shim, H. K.; Park, M. J.; Hwang, D. H.; Jung, B. J. *Macromolecules* **2006**, *39*, 177.
(3) Thompson, B. C.; Kim, Y.-G.; Reynolds, J. R. *Macromolecules* **2005**, *38*, 5359.
(4) Sun, X. B.; Zhou, Y. H.; Wu, W. C.; Liu, Y. Q.; Tian, W. J.; Yu, G.; Qiu, W. F.; Chen, S. Y.; Zhu, D. B. *J. Phys. Chem. B* **2006**, *110*, 7702.
(5) Shaheen, S. E.; Brabec, C. J.; Sariciftci, N. S.; Padinger, F.; Fromherz, T.; Hummelen, J. C. *Appl. Phys. Lett.* **2001**, *78*, 841.
(6) Vissenberg, M. C. J. M.; Blom, P. W. M. *Synth. Met.* **1999**, *102*, 1053.
(7) Mihailetchi, V. D.; van Duren, J. K. J.; Blom, P. W. M.; Hummelen, J. C.; Janssen, R. A. J.; Kroon, J. M.; Rispens, M. T.; Verhees, W. J. H.; Wienk, M. M. *Adv. Funct. Mater.* **2003**, *13*, 43.
(8) Zhou, E. J.; Tan, Z. A.; Huo, L. J.; He, Y. J.; Yang, C. H.; Li, Y. F. *J. Phys. Chem. B.* **2006**, *110*, 26062.
(9) Zhou, E. J.; Tan, Z. A.; Yang, C. H.; Li, Y. F. *Macromol. Rapid. Commum.* **2006**, *27*, 793.
(10) Hou, J. H.; Tan, Z. A.; Yan, Y.; He, Y. J.; Yang, C. H.; Li, Y. F. J. *Am. Chem. Soc.* **2006**, *128*, 4911.
(11) Zhan, X.; Tan, Z.; Domercq, B.; An, Z.; Zhang, X.; Barlow, S.; Li, Y.; Zhu, D.; Kippelen, B.; Marder, S. R. J. *Am. Chem. Soc.* **2007**, *129*, 7246.
(12) Zou, Y.; Wu, W.; Sang, G.; Yang, Y.; Liu, Y.; Li, Y. *Macromolecules* **2007**, *40*, 7231.
(13) Cravino, A.; Roquet, S.; Aleveque, O.; Leriche, P.; Frere, P.; Roncali, J. *Chem. Mater.* **2006**, *18*, 2584.
(14) Shu, C. F.; Dodda, R.; Wu, F. I.; Liu, M. S.; Jen, A. K. Y. *Macromolecules* **2003**, *36*, 6698.
(15) Lin, X. Q.; Chen, B. J.; Zhang, X. H.; Lee, C. S.; Kwong, H. L.; Lee, S. T. *Chem. Mater.* **2001**, *13*, 456.
(16) Shirota, Y. *Mater. Chem.* **2000**, *10*, 1.
(17) Cravino, A.; Roncali, J.; Leriche, P.; Aleveque, O.; Roquet, S. *Adv. Mater.* **2006**, *18*, 3033.
(18) Pu, Y. J.; Soma, M.; Kido, J. J.; Nishide, H. *Chem. Mater.* **2001**, *13*, 3817.
(19) He, C.; He, Q.; Yang, X.; Wu, G.; Yang, C.; Bai, F. L.; Shuai, Z.; Wang, L.; Li, Y. J. *Phys. Chem. C.* **2007**, *111*, 8661.
(20) Roquet, S.; Cravino, A.; Leriche, P.; Aleveque, O.; Frere, P.; Roncali, J. J. *Am. Chem. Soc.* **2006**, *128*, 3459.
(21) He, C.; He, Q. G.; He, Y. J.; Li, Y. F.; Bai, F. L.; Yang, C. H.; Ding, Y. Q.; Wang, L. X.; Ye, J. P. *Sol. Energy. Mater. Sol. Cells* **2006**, *90*, 1815.
(22) Pu, Y. J.; Takashi, K.; Minoru, S.; Kido, J. J.; Iroyuki, N. *Synth. Met.* **2004**, *143*, 207.
(23) Liao, L.; Pang, Y.; Ding, L.; Karasz, F. E. *Macromolecules* **2001**, *34*, 6756.
(24) Tokito, S.; Tanaka, H.; Noda, K.; Okada, A.; Taga, Y. *Appl. Phys. Lett.* **1997**, *70*, 1929.
(25) Li, X. Z.; Zeng, W. J.; Zhang, Y.; Hou, Q.; Yang, W.; Cao, Y. *Eur. Polym. J.* **2005**, *41*, 2923.
(26) Agrawal, A. K.; Jenekhe, S. A. *Chem. Mater.* **1996**, *8*, 579.
(27) Chen, W. C.; Liu, C. L.; Yen, C. T.; Tasi, F. C.; Tonzola, C. J.; Olson, N.; Jenekhe, S. A. *Macromolecules* **2004**, *37*, 5959.
(28) Ravirajan, P.; Haque, S. A.; Durrant, J. R.; Bradley, D. D. C.; Nelson, J. *Adv. Funct. Mater.* **2005**, *15*, 609.
(29) Blom, P. W. M.; Mihailetchi, V. D.; Koster, L. J. A.; Markov, D. E. *Adv. Mater.* **2007**, *19*, 1551.
(30) Liu, J. S.; Tanaka, T.; Sivula, K.; Alivisatos, A. P.; Frechet, J. M. J. J. *Am. Chem. Soc.* **2004**, *126*, 6550.
(31) Tan, S. T.; Zou, Y. P.; Zhu, W. G.; Jiang, C. Y. *Opt. Mater.* **2006**, *28*, 1108.
(32) Tang, W. H.; Lin, K.; Tan, L. W.; Lin, T. T.; Kietzke, T.; Chen, Z. K. *Macromolecules* **2007**, *40*, 6164.

MA800847F